Anal. Chem. **2007,** *79,* 8494−8501

Versatile Immunosensor Using CdTe Quantum Dots as Electrochemical and Fluorescent Labels

Rongjing Cui, Hong-Cheng Pan, Jun-Jie Zhu,* and Hong-Yuan Chen

Key Lab of Analytical Chemistry for Life Science (MOE), School of Chemistry and Chemical Engineering, Nanjing University, Nanjing 210093, People's Republic of China

A versatile immunosensor using CdTe quantum dots as electrochemical and fluorescent labels has been developed for sensitive protein detection. This sandwich-type sensor is fabricated on an indium tin oxide chip covered with a well-ordered gold nanoparticle monolayer. Gel imaging systems were successfully introduced to develop a novel high-efficient optical immunoassay, which could perform simultaneous detection for the samples with a series of different concentrations of a target analyte. The linear range of this assay was between 0.1 and 500 ng/mL, and the assay sensitivity could be further increased to 0.005 ng/mL with the linear range from 0.005 to 100 ng/mL by stripping voltammetric analysis. The immunosensor showed good precision, high sensitivity, acceptable stability, and reproducibility and could be used for the detection of real sample with consistent results in comparison with those obtained by the ELISA method.

Recently, the applications based on nanoparticles (NPs) in immunoassay have attracted wide interest due to their unique optical, electronic, and mechanic properties. Various NPs such as gold, silver, silica, and quantum dots (QDs)[1−7] have been extensively used for ultrasensitive optical and electrochemical bioassays. Among them, QDs have shown great potential because of their unique advantages: nanoscale size similar to proteins, broad excitation spectra for multicolor imaging, robust, narrow-band emission, and versatility in surface modification. Stable, water-soluble QDs permit surface modification with various biomolecules such as peptides, oligonucleotides, and proteins for in vitro and in vivo targeting, labeling, and imaging applications.[8−14] On the other hand, the QDs-based electrochemical bioassay has also become a favorite topic because of inherent miniaturization, high sensitivity, low cost, and low power requirements. A series of QDs such as CdS, PbS, CuS, and ZnS[15−18] was developed for sensitive electrochemical detection of multiple proteins and DNA target analytes in connection with voltammetric detection of the metal components. However, the synthesis of such QDs labels may be time- and cost-consuming and still complicated. The QDs-based western blot technology for protein detection has been reported[19,20] by using gel imaging systems. The imaging systems have a broad bandwidth UV light to excite QDs labels and obtain a highly stable fluorescent emission. It might be an interesting candidate for the detection of a QDs labeled bioassay due to its several advantages over the conventional detection systems. The gel imaging can carry out rapid analysis for a large number of samples in a single experiment. Moreover, the amount of material required is significantly small, and reaction volumes are lower than the amount that is typically used in conventional microtiter plates.

In the field of biosensors, stability and activity of the immobilized biocomponents on solid support have been a long-standing goal. Among various immobilized matrixes adopted, the self-assembled monolayer (SAM) offers a means to control its physical and chemical properties in biosensing applications. Furthermore, the uniformity of SAMs enables position-selective immobilization of biomolecules and prevents nonspecific interactions. Gold nanoparticle (GNP) is of special interest in the wide application of a molecular self-assembly matrix for loading of

* To whom correspondence should be addressed. Fax: +86-25-83594976. E-mail: jjzhu@netra.nju.edu.cn.

(1) Authier, L.; Grossiord, C.; Brossier, P.; Limoges, B. *Anal. Chem.* **2001**, *73*, 4450−4456.
(2) Wang, J.; Xu, D.; Kawde, A.; Polsky, R. *Anal. Chem.* **2001**, *73*, 5576−5581.
(3) Cai, H.; Xu, Y.; Zhu, N.; He, P.; Fang, Y. *Analyst* **2002**, *127*, 803−808.
(4) Chan, W. C. W.; Nie, S. M. *Science* **1998**, *281*, 2016−2018.
(5) Mattoussi, H.; Mauro, J. M.; Goldman, E. R.; Anderson, G. P.; Sundar, V. C.; Mikulec, F. V.; Bawendi, M. G. *J. Am. Chem. Soc.* **2000**, *122*, 12142−12150.
(6) Parak, W. J.; Gerion, D.; Pellegrino, T.; Zanchet, D.; Micheel, C.; Williams, S. C.; Boudreau, R.; Le Gros, M. A.; Larabell, C. A.; Alivisatos, A. P. *Nanotechnology* **2003**, *14*, R15−R27.
(7) Shipway, A. N.; Katz, E.; Willner, I. *Chem. Phys. Chem.* **2000**, *1*, 18−52.
(8) Dabbousi, B. O.; RodriguezViejo, J.; Mikulec, F. V.; Heine, J. R.; Mattoussi, H.; Ober, R.; Jensen, K. F.; Bawendi, M. G. *J. Phys. Chem. B* **1997**, *101*, 9463−9475.
(9) Goldman, E. R.; Balighian, E. D.; Kuno, M. K.; Labrenz, S.; Tran, P. T.; Anderson, G. P.; Mauro, J. M.; Mattoussi, H. *Phys. Status Solidi B* **2002**, *229*, 407−414.
(10) Wolcott, A.; Gerion, D.; Visconte, M.; Sun, J.; Schwartzberg, A.; Chen, S. W.; Zhang, J. Z. *J. Phys. Chem. B* **2006**, *110*, 5779−578.
(11) Jaiswal, J. K.; Mattoussi, H.; Mauro, J. M.; Simon, S. M. *Nat. Biotechnol.* **2003**, *21*, 47−51.
(12) Jaiswal, J. K.; Simon, S. M. *Trends Cell. Biol.* **2004**, *14*, 497−504.
(13) Ballou, B.; Lagerholm, B. C.; Ernst, L. A.; Bruschez, M. P.; Waggoner, A. S. *Bioconjugate Chem.* **2004**, *15*, 79−86.
(14) Dahan, M.; Le'vi, S.; Luccardini, C.; Rostaing, P.; Riveau, B.; Triller, A. *Science* **2003**, *302*, 442−445.
(15) Hansen, J. A.; Mukhopadhyay, R.; Hansen, J.; Gothelf, K. V. *J. Am. Chem. Soc.* **2006**, *128*, 3860−3861.
(16) Hansen, J. A.; Wang, J.; Kawde, A.-N.; Xiang, Y.; Gothelf, K. V.; Collins, G. *J. Am. Chem. Soc.* **2006**, *128*, 2228−2229.
(17) Liu, G.; Wang, J.; Kim, J.; Jan, M. R. *Anal. Chem.* **2004**, *76*, 7126−7130.
(18) Wang, J.; Liu, G.; Merkoci, A. *J. Am. Chem. Soc.* **2003**, *125*, 3214−3215.
(19) Bakalova, R.; Zhelev, Z.; Ohba, H.; Baba, Y. *J. Am. Chem. Soc.* **2005**, *127*, 9328−9329.
(20) Ornberg, R. L.; Harper, T. F.; Liu, H. *Nat. Methods* **2005**, *2*, 79−81.

10.1021/ac070923d CCC: $37.00 © 2007 American Chemical Society
Published on Web 10/10/2007

biomolucules.[21−23]The GNP SAM on indium tin oxide (ITO) has been demonstrated for a hydrogen peroxide sensor.[24]

Herein, we used a simple and facile synthetic strategy to prepare uniform-size and highly luminescent water-soluble CdTe QDs and fabricated a versatile immunosensor to effectively detect protein based on the CdTe QDs label simultaneously as fluorescent and electrochemical signals. In the case of the preparation of the versatile immunosensor, the goat anti-human IgG antibody (Ab_1) was immobilized on the ITO chip coated with well-ordered GNP. The analytical procedure consists of the immunoreaction of the antigen (Ag) with Ab_1, followed by binding CdTe QDs-labeled mouse anti-human IgG antibody (CdTe QDs−Ab_2). Formation of an Ab layer and the Ag−Ab complexes on the chip was characterized by atomic force microscopy (AFM), electrochemical impedance spectroscopy (EIS), fluorescence microscopy image, stripping voltammetry, and gel imaging systems. The detailed optimization and attractive performance characteristics of the developed versatile immunoassay are reported in the following sections.

EXPERIMENTAL SECTION

Regents and Buffers. All stock solutions were prepared using deionized or autoclaved water. ITO-coated glass slides, which had a surface resistance of 30−60 Ω/cm^2, were purchased from Condue Optics and Electronics Technology Co., Ltd. (Jintan, China). The ITO chip with 4 mm diameter was used to the Ab−Ag reaction area. Human IgG, goat anti-human IgG, monoclonal mouse anti-human IgG and bovine serum albumin (BSA) were purchased from Shanghai Huamei Biochemical Reagents (Shanghai, China). Skim milk was purchased from Shanghai Guangming Co. (Shanghai, China). 1-Ethyl-3-(3-dimethylaminopropyl) carbodiimide hydrochloride (EDC) and 3-mercaptopropionic acid (MPA; >99%) were purchased from Sigma−Aldrich. KBH_4 (96%), tellurium powder (99.999%), chloroauric acid ($HAuCl_4$), and trisodium citrate were obtained from Shanghai Reagent Co. (Shanghai, China). Poly(diallyldimethylammonium chloride) (PDDA; 20%, w/w in water, MW = 200 000−350 000), Disodium hydrogen phosphate, Potassium dihydrogen phosphate, and sodium hydroxide were obtained from Nanjing Chemical Reagents Factory (Nanjing, China). All other chemicals were of analytical grade and were used as received. The ultrafiltration filter (Millipore Corp.) was used to separate and concentrate the sample solution. Gold nanoparticles were prepared by citrate reduction of $HAuCl_4$ in aqueous solution.[25]

Preparation of Water-Soluble CdTe QDs. CdTe QDs were synthesized according to the modifications of a literature procedure.[26,27] Briefly, 198 mL of doubly distilled water was degassed by bubbling nitrogen for ~1 h. $CdCl_2{\cdot}2.5H_2O$ (0.1142 g, 0.5 mM) and MPA (0.0849 g, 0.8 mM) were added into the aqueous solution, and the pH was adjusted to 8.0−8.5 by the addition of a 5% NaOH solution. Nitrogen was further bubbled through the solution for ~30 min. Subsequently, 2.0 mL of freshly prepared NaHTe solution produced by the reaction of KBH_4 (0.0480 g, 0.89 mM) with tellurium powder (0.0480 g, 0.375 mM) in a 2.0-mL aqueous solution was mixed with above $CdCl_2$−MPA solution. The resulting mixture solution was refluxed under nitrogen flow at 96−99 °C for 3 h to obtain CdTe QDs with an emission maximum at 620 nm.

The obtained QDs solution was further purified by ultrafiltration according to the previous report.[28] The first step was carried out on 3000 MW size filter and centrifugation at 3000*g* for 15 min at 4 °C to remove nonreacted MPA. The QDs were washed three times with 50 mM PBS in pH 7.4. The upper phase was decanted, dissolved in PBS, and subjected additionally to a second ultrafiltration step on a 50 000 MW filter. After the second ultrafiltration step, the lower phase was concentrated on a 3000 MW filter to reach a concentration of corresponding to 0.05 mM QDs.[29] The purified water-soluble QDs possessed a bright fluorescence and a good stability in a buffer.

Bioconjugation of CdTe QDs with Antibodies. The conjugation procedure of CdTe QDs with Ab_2 was similar to previous reports.[30,31] One milliliter of CdTe QDs solution after purification was mixed with 200 μL of Ab_2 solution containing 0.4 mg of antibody in 200 μL of PBS, pH 7.4. Then 150 μL of freshly prepared 4.2 mg/mL EDC stock solution was added to the mixture. The samples were incubated 2 h at room temperature under shaking in the dark and kept overnight at 4 °C. The free nonconjugated QDs as well as the isourea byproduct of the conjugation reaction were removed by ultrafiltration. A 1.35-mL aliquot of the above mixture was subjected to ultrafiltration using a 50 000 MW filter; after the lower phase was removed, the upper phase containing QDs−antibody conjugations was decanted, diluted to 1.5 mL with PBS, and then 0.5 mL of 50 mM PBS with 1% BSA was added. The solution was stored at 4 °C.

Preparation of GNP Monolayer on ITO Chip. The immunoassay was performed on an ITO chip coated with GNP monolayer. Before modification, the ITO chips were cleaned with acetone, ethanol, and water. After being immersed in a solution of 1:1 (v/v) ethanol/NaOH (1 M) for 15 min, they were rinsed with water. The chips were dipped in a 0.05% PDDA aqueous solution (pH 7.0) for 20 min to modify a monolayer of PDDA. After the coupling reaction, the modified substrates were removed from the solution and rinsed several times with water to remove the physically adsorbed PDDA. Then the substrates were dried under a stream of nitrogen. Prepared in this way, the surface of the substrate was covered with positively charged PDDA that readily adsorbed GNPs with negative charge. The modified ITO was immersed in the GNP solution for 20 min. After the modified ITO chips were dried under a stream of nitrogen, a 3-mm-thick poly(dimethylsiloxane) with a circular opening of 4-mm diameter was formed from a predefined mold and was bound to the ITO surface to form the Ab−Ag reaction area. The

(21) Brown, K. R.; Fox, A. P.; Natan, M. J. *J. Am. Chem. Soc.* **1996**, *118*, 1154−1157.
(22) Willner, I.; Lapidot, N.; Riklin, A.; Kasher, R.; Zahavy, E.; Katz, E. *J. Am. Chem. Soc.* **1994**, *116*, 1428−1441.
(23) Dequarie, M.; Degrand, C.; Limoges, B. *Anal. Chem.* **2000**, *72*, 5521−5528.
(24) Wang, L.; Wang, E. *Electrochem. Commun.* **2004**, *6*, 225−229.
(25) Enustun, B. V.; Turkevich, J. *J. Am. Chem. Soc.* **1963**, *85*, 3317−3328.
(26) Qian, H. F.; Dong, C. Q.; Weng, J. F.; Ren, J. C. *Small* **2006**, *2*, 747−751.
(27) Zhang, H.; Wang, D.; Yang, B.; Möhwald, H. *J. Am. Chem. Soc.* **2006**, *128*, 10171−10180.
(28) Zhelev, Z.; Bakalova, R.; Ohba, H.; Jose, R.; Imai, Y.; Baba, Y. *Anal. Chem.* **2006**, *78*, 321−330.
(29) Yu, W. W.; Qu, L.; Guo, W.; Peng, X. *Chem. Mater.* **2003**, *15*, 2854−2860.
(30) Zhelev, Z.; Ohba, H.; Bakalova, R.; Jose, R.; Fukuoka, S.; Nagase, T.; Ishikawa, M.; Baba, Y. *Chem. Commun.* **2005**, *15*, 1980−1982.
(31) Wang, S. P.; Mamedova, N.; Kotov, N. A.; Chen, W.; Studer, J. *Nano Lett.* **2002**, *2*, 817−822.

Scheme 1. Analytical Procedure of Fluorescent and Electrochemical Immunoassay Based on CdTe QDs Label

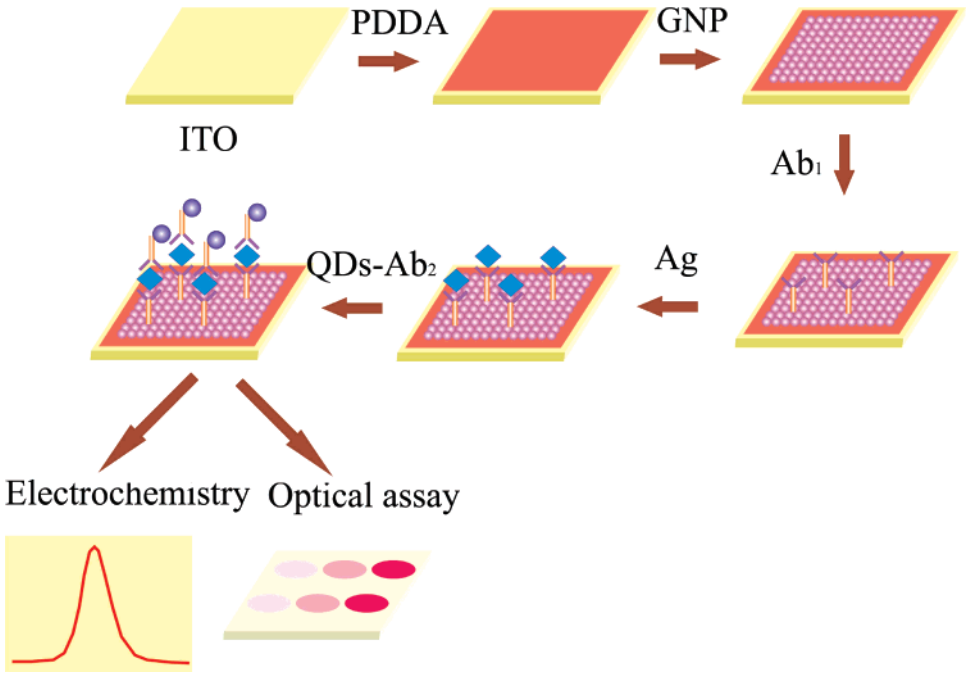

construction of the chip support was shown in Scheme 1. All resulting chips were washed with water and stored at 4 °C when not in use.

Antibody Immobilization and Immunoreaction Procedure. Ab_1 was immobilized onto the GNP-modified ITO chip. A10-μL aliquot of 0.4 mg/mL antibody solution (50 mM PBS, pH 6.0) was spread onto the chip surface. The chips were incubated at 4 °C in a moisture chamber overnight. After incubation, they were rinsed with PBS, 0.05% Tween to remove physically adsorbed Ab_1. The chips were then blocked with 5% skim milk solution for 1 h at room temperature and washed with PBS. After aspiration, Ab_1-modified chips incubated with 10 μL of detecting human IgG (HIgG) samples for 50 min at 37 °C. By the binding reaction between Ab_1 and HIgG on the chips, 10 μL of CdTe QDs−Ab_2 was spotted onto a certain region of the chip. After an incubation of 50 min, the chips were washed thoroughly with water to remove nonspecifically bound CdTe QDs conjugations, which could cause a background response before measurement. The way to the immobilization of Ab_1 and the immunoassay procedure are also shown in Scheme 1.

AFM Imaging. All AFM experiments were performed on SPA-300 HV with a SPI 3800 controller (Seiko). They were carried out using the tapping mode. All images are presented without any subsequent data processing. All chips were washed thoroughly using water and were measured in air.

Electrochemical Impedance Spectroscopy. The EIS analyses were performed with an Autolab PGSTAT12 (Ecochemie, BV, The Netherlands) and controlled by GPES 4.9 and FRA 4.9 softwares. All experiments were carried out using a conventional three-electrode system with ITO chip as the working electrode, a platinum wire as the auxiliary electrode, and a saturated calomel electrode (SCE) as the reference electrode. The electrochemical impedance spectra were recorded in the frequency range $0.1-1.0\times10^5$ Hz, at the formal potential of the $Fe(CN)_6^{3-/4-}$ redox couple and with a perturbation potential of 5 mV.

Optical Detection. Fluorescence microscopy images were taken from a Nikon TE2000-U inverted optical microscope. Optical immunoassay was performed using gel image systems (Bio-Rad). The relative intensity of each dot was scored using Quantity One (Bio-Rad),[32,33] a quantitative analysis software program.

Stripping Voltammetric Analysis. The CdTe QDs remaining at the chip surface were dissolved by the addition of 100 μL of 0.10 M HNO_3 solution. The solution was transferred into 900 μL of 0.20 M acetate buffer at pH 4.6; the amount and identity of the dissolved metal ions were determined by electrochemical stripping techniques. The square wave stripping voltammetric analysis (SWSV) was conducted using a CHI660 electrochemical workstation equipped with a stirring machine (CH Instruments Inc). The three-electrode system used for running the SWSV consisted of a glassy carbon working electrode, SCE, and a platinum counter electrode. The electrochemical procedure involved a 1-min pretreatment at +0.6 V, 10-min electrodeposition at −1.00 V, and stripping from −1.00 to −0.45 V using a square wave voltammetric waveform, with 4-mV potential steps, 25-Hz frequency, and 25-mV amplitude.

RESULTS AND DISCUSSION

Preparation and Characterization of ITO Chips. (a) AFM Imaging. Figure 1 presents the images of the surfaces of the ITO modified with GNP monolayer and Ab_1 immobilized on the monolayer. Figure 1a significantly indicated that the formation of the GNP monolayer was accomplished on the ITO surface, and the monolayer was complete, homogeneous, and well ordered.

(32) Marko-Varga, G.; Berglund, M.; Malmstrom, J.; Lindberg, H.; Fehniger, T. E. *Electrophoresis* **2003**, *24*, 3800−3805.
(33) Chubinskaya, S.; Mikhail, R.; Deutsch, A.; Tindal, M. H. *J. Histochem. Cytochem.* **2001**, *49*, 1165−1176.

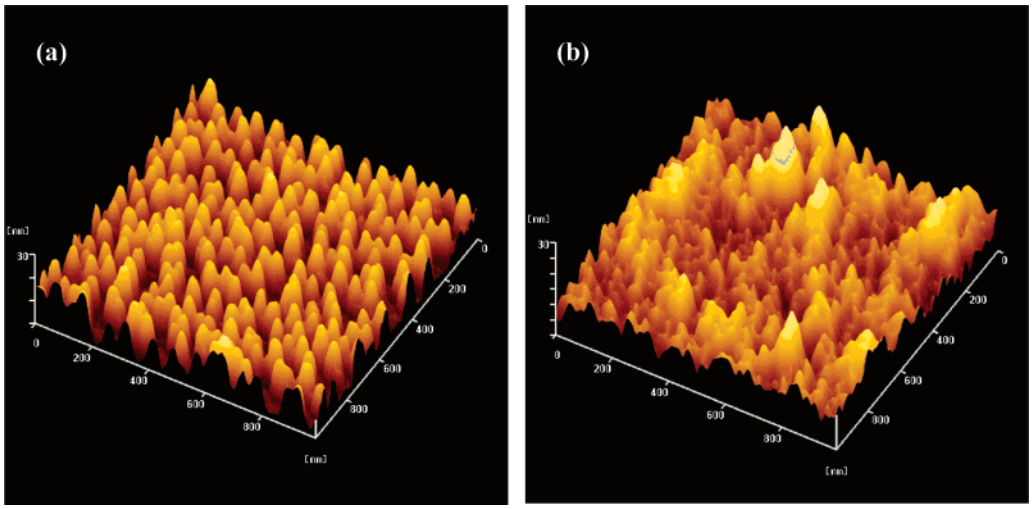

Figure 1. (a) AFM image of the GNP monolayer on the ITO chip surface. (b) AFM image of the Ab_1 immobilized on the ITO chip coated with GNP monolayer.

According to the previous reports,[34] the main interaction of successive multiple ionic layers was ionic interaction. The ITO surface was coated with a large number of hydroxy groups. PDDA was a quaternary ammonium polyelectrolyte, which was easily protonated and retained positive charge. The ionic interactions not only resulted in the strong combination of PDDA with the hydroxy groups on the ITO surface but also made PDDA combine with negatively charged GNPs.[35,36] The value of pI of IgG was close to 7.0, and therefore, in a solution at pH 6.0, Ab_1 should bear a net positive charge. When the Ab_1 in pH 6.0 solutions was spotted onto the GNP surfaces, it could be firmly attached onto the surfaces through ionic interactions and other interaction between GNPs and mercapto or primary amine groups of biomolecules.[37] Figure 1b shows the AFM image of Ab_1 layers formed after the reaction between Ab and GNPs overnight at 4 °C. The Ab_1 layer was not absolutely a monolayer, and a few aggregates of the Ab could still be observed on the surface even though the Ab_1-modified surface was thoroughly rinsed. Making a comparison between panels a and b in Figure 1, the distinctive difference in the topography can be observed before and after the binding of Ab_1. This feature indicated that Ab_1 was linked to the chip surface.

(b) Electrochemical Impedance Measurements. Impedance spectroscopy was reported as an effective method to monitor the surface features allowing the understanding of chemical transformation and processes associated with the conductive electrode surface.[38] The impedance spectra include a semicircular portion and a linear portion, the semicircular portion at higher frequencies corresponds to the electron-transfer-limited process, and the linear part at lower frequencies corresponds to the diffusion process. The semicircle diameters correspond to the electron-transfer resistance (R_{et}). Figure 2 shows the Nyquist plots

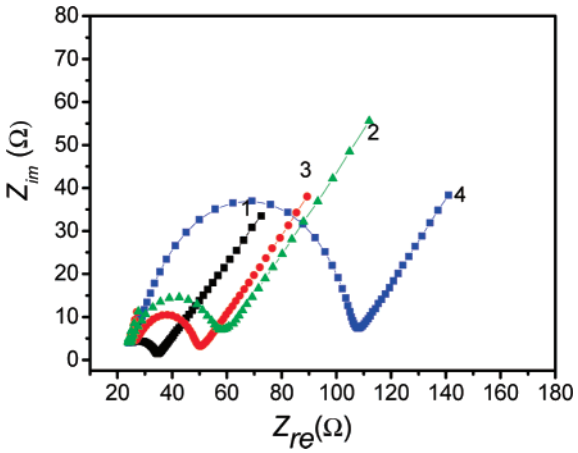

Figure 2. Nyquist diagrams for the electrochemical impedance measurements of ITO chips in a solution of 0.1 M KNO_3 containing 5 mM $Fe(CN)_6^{3-}$ and 5 mM $Fe(CN)_6^{4-}$. (1) Bare ITO chip, (2) PDDA/ITO chip, (3) GNP/PDDA/ITO chip, and (4) Ab_1/GNP/PDDA/ITO chip.

of EIS for the bare ITO chip, PDDA/ITO, GNP/PDDA/ITO, and Ab_1/GNPs/PDDA/ITO. All modified chips showed the large increase in diameter compared to that of the bare ITO chip, indicating much higher R_{et} values. Because PDDA is nonconductive, its monolayer film blocks the electron transfer of redox probe $[Fe(CN)_6]^{3-/4-}$ and R_{et} increase.[39] The chip modified with GNPs showed a lower R_{et} compared to that of a PDDA covering on chip because of the contribution of assembled GNPs. Additionally, the Ab_1-immobilized ITO chip showed the greatest increase in diameter, suggesting that Ab_1 layer formed an additional barrier and further prevented the redox probe to the electrode surface. The results were consistent with the AFM image as shown in Figure 1b.

Bioactivity Detection of CdTe QDs−Ab_2 Conjugation. The water-soluble CdTe QDs were chosen to develop versatile nanopaticle labels for optical and electrochemical immunoassay. The carboxyl groups linked with CdTe QDs provide a facile route to couple to biomolecules with amine groups. EDC[28] is a commonly used coupling agent that can link between amine groups of

(34) Katayama, H.; Ishihama, Y.; Asakawa, N. *Anal. Chem.* **1998**, *70*, 2254−2260.
(35) Liu, Y.; Fanguy, J. C.; Bledsoe, J. M.; Henry, C. S. *Anal. Chem.* **2000**, *72*, 5939−5944.
(36) Wang, W.; Zhao, L.; Zhang, J. R.; Zhu, J-J. *J. Chromatogr., A* **2006**, *1136*, 111−117.
(37) Zhao, J.; Henkens, R. W.; Stonehuerner, J.; O_Daly, J. P.; Crumbliss, A. L. *J. Electroanal. Chem.* **1992**, *327*, 109−119.
(38) Bard, A. J.; Faulkner, L. R.; *Electrochemical Methods: Fundamentals and Applications*; Wiley: New York, 1980.
(39) Zhao, W.; Xu, J. J.; Chen, H. Y. *Front. Biosci.* **2005**, *10*, 1060−1069.

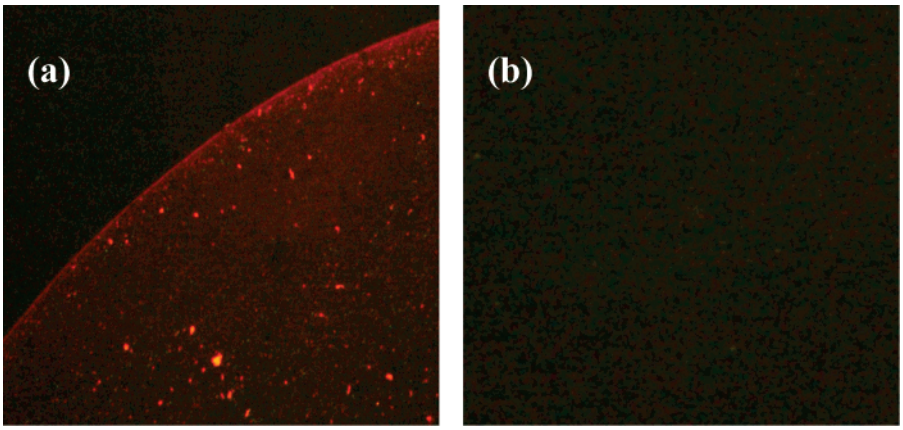

Figure 3. (a) Fluorescence microscopy image of HIgG-coated ITO chip incubated with the CdTe QDs−Ab_2 under UV illumination. (b) Fluorescence microscopy image of the HIgG-coated ITO chip incubated with CdTe QDs.

proteins and carboxylic groups of some compounds. Here, EDC was chosen to conjugate Ab_2 with CdTe QDs, followed by ultrafiltration to remove the free nonconjugated QDs and the isourea byproduct of the conjugation reaction. Bioactivity and specificity after conjugation was confirmed by the Ag−Ab_2 recognition reaction that occurred between Ag and CdTe QDs−Ab_2 conjugates. Therefore, HIgG was first immobilized on the ITO chips modified with a GNP monolayer according to the same procedure of the immobilization of Ab_1. After blocking with skim milk solution, HIgG-modified ITO chips were used to attach the CdTe QDs−Ab_2. The binding reactions were allowed to continue for 50 min at 37 °C. Figure 3a shows a typical fluorescence microscopy image of the HIgG-modified chip incubated with the CdTe QDs−Ab_2. A strong red fluorescence was observed at the HIgG-coated area, indicating that the CdTe QDs−Ab_2 was successfully attached to the chip through the Ag−Ab interaction. In contrast, no fluorescence was observed with a control HIgG-modified ITO incubated with CdTe QDs solution (Figure 3b), which confirmed that nonspecific adsorption was negligible. The above experimental results showed that the prepared CdTe QDs−Ab_2 conjugation could be used as labels for bioassay applications.

Sandwich Immunoassay on the ITO Chip. The application of CdTe QDs−Ab_2 conjugation was further studied in the sandwich fluorescent and electrochemical immunoassay. The sandwich immunoassay was performed with the GNP monolayer-modified ITO chip (Scheme 1). The Ab_1 was first immobilized on the chip, and then the HIgG was bound to Ab_1 after blocking with 5% skim milk solution, followed by the interaction with CdTe QDs−Ab_2. The procedure for this sandwich immunoassay was described in the Experimental Section. Two applications were demonstrated to detect the target HIgG. First, we investigated a fluorescent immunoassay with gel imaging systems. QDs are extremely efficient at absorbing UV light and converting it to highly stable fluorescent emission, making them up to 50× brighter than conventional organic fluorophores.[20] Most gel imagers have a source sufficient to excite QDs conjugates, such as an epi-UV illuminator. Figure 4a shows the fluorescence image of gel imaging systems on the ITO chip with increase of HIgG concentration. The relative amount of each result was scored using Quantity One (Bio-Rad).[40,41] We could observe that the fluorescence intensity of the Ab-spotted area increased with the increase of HIgG concentration from 0.1 to 500 ng/mL (B−F), which showed the good quantitative results with the detection limit as low as 0.03 ng/mL ($n = 3$, 0.187 pM). Control experiment (A) in Figure 4a represents the assay taken through the full procedure without exposure to Ag. The other control experiment (A′) is taken through full immunoassay using Ab_2 instead of QDs−Ab_2 omitting addition HIgG. The response in each case was much smaller than that of the immunosensor at the lowest concentration of HIgG, and control (A) was only a little larger than that of control (A′) without QDs. Thus, the nonzero background signal resulted from the sum of the residual nonspecific binding and modified ITO chip. In order to avoid any effects of changes in instrument and system, it was necessary to take out the nonzero signal from the detection results of samples. In addition, inhibition of nonspecific binding was critical to achieve the best sensitivity and detection limits. Thus, we developed an effectively blocking step with 5% skim milk; that is, the skim milk was adsorbed onto the ITO surfaces after the Ab_1 immobilization process. The adsorption of skim milk onto the ITO chip was characterized by AFM studies. Figure 5 shows an AFM image of GNP monolayer on the ITO surface blocked with 5% skim milk. It was found that many small biomolecules formed a compact thin film to cover on the chip. Few aggregates of biomolecules could be observed on the surface after it was thoroughly rinsed. The result indicated the skim milk could block the nonspecific binding activities. In previous reports, BSA was the most commonly used blocking reagent that could lower the nonspecific binding activities in the immunoassay. Comparable immunoassays were performed with a 5% BSA solution blocking under the same conditions. The result showed that the skim milk blocking method was superior to the traditional BSA blocking method for preventing buildup of the background signal. The intra-assay precision was estimated from a series of five repetitive measurements of samples containing 0.1, 200, and 500 ng/mL HIgG that yielded the relative standard deviations (RSD) of 7.1, 6.5, and 6.9%, respectively. The interassay precision, or the fabrication reproducibility, was estimated by determining the HIgG

(40) Marko-Varga, G.; Berglund, M.; Malmstrom, J.; Lindberg, H.; Fehniger, T. E. *Electrophoresis* **2003**, *24*, 3800−3805.
(41) Chubinskaya, S.; Mikhail, R.; Deutsch, A.; Tindal, M. H. *J. Histochem. Cytochem.* **2001**, *49*, 1165−1176.

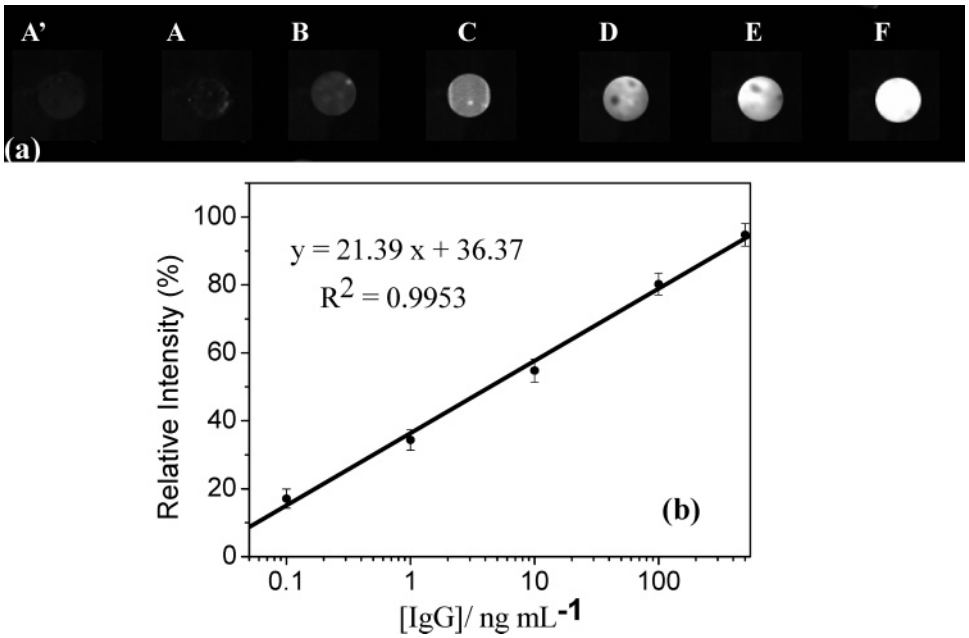

Figure 4. (a) Fluorescence images of gel imaging systems on the ITO chips for different HIgG levels (from A to F: 0, 0.1, 1.0, 10, 100, and 500 ng mL^{-1} HIgG, respectively). (A′) Full immunoassay using Ab_2 instead of QDs−Ab_2 omitting addition HIgG. (b) Detection curve for HIgG plotted on a semilog scale.

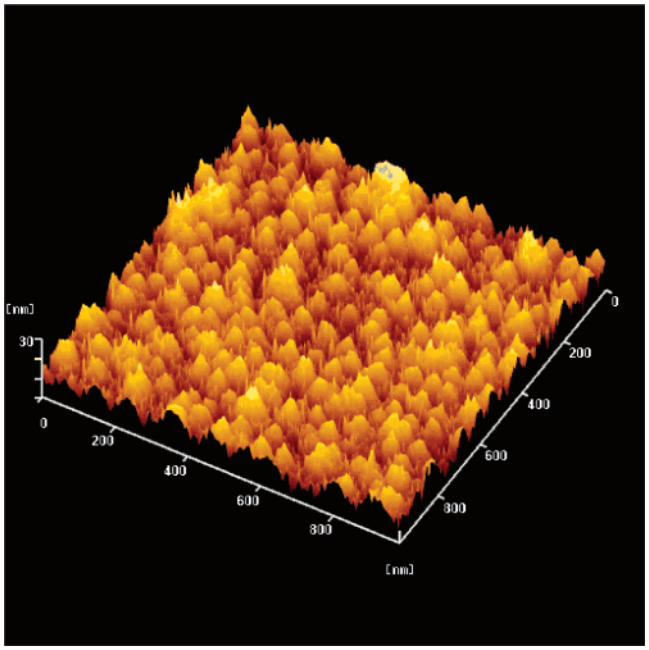

Figure 5. AFM image of GNP monolayer on the ITO surface blocked with 5% skim milk.

level with five immunosensors made at the same ITO independently. The RSD of interassay using this method was 5.2% at the HIgG concentration of 10 ng/mL.

In addition to optical assay, the target protein−HIgG on the ITO chip was also detected with electrochemical measurement as shown in Figure 6. The CdTe QDs as described above could be dissolved, and the dissolved cadmium ions were determined by SWSV. The electrochemical signal was directly proportional to the amount of analyte (HIgG). Figure 6a shows the typical square wave voltammograms. The voltammetric peaks were well defined, and the intensity was proportional to the concentration of the corresponding HIgG. The resulting calibration plots were linear as shown in Figure 6b; the correlation coefficients was 0.995. The corresponding calibration plot of response versus [HIgG] was linear over the 0.005∼100 ng/mL range and was suitable for quantitative analysis. The response obtained with a protein target concentration of 5.0 pg/mL indicated a detection limit of ∼1.5 pg/mL (9.3 fM). The low detection compared favorably with the values obtained with an enzyme-linked immunosorbent assay[42] (ELISA, 40 pg/mL) and GNP-labeled immunosensor (3.0 pM).[23] The high sensitivity was coupled with excellent selectivity and the absence of nonspecific adsorption effects. The behavior was attributed to the following reasons. The ITO chips coated with a well-ordered GNP monolayer offered a congenial microenvironment similar to that of protein in a native system and allowed the protein molecules more freedom in orientation, which provided stereo attaching sites and an ideal and effective platform for the immobilization of Ab_1. The second reason was a blocking step mentioned above. In particular, the sandwich immunoassay was based on CdTe QDs labels as electrochemical signal by stripping analysis. Stripping analysis is a powerful technique for trace metal measurements. Its remarkable sensitivity is attributed to the preconcentration step, during which the target metals are accumulated onto the working electrode. A series of five repetitive measurements with HIgG concentration of 0.05, 50.0, and 100 ng/mL yielded reproducible cadmium signals with the RSD of 6.1, 5.6, and 5.9%, respectively.

Application of the Versatile Immunosensor in Human Serum. The feasibility of the immunoassay for clinical applications was investigated by analyzing several real samples, in comparison with the ELISA method. These serum samples were diluted to different concentrations with pH 7.0 PBS. Figure 7 describes the

(42) Scuderi, P.; Sterling, K. E.; Lam, K. S.; Finley, P. R.; Ryan, K. J.; Ray, C. G.; Petersen, E.; Slymen, D. J.; Salmon, S. E. *Lancet* **1986**, *2*, 1364−1365.

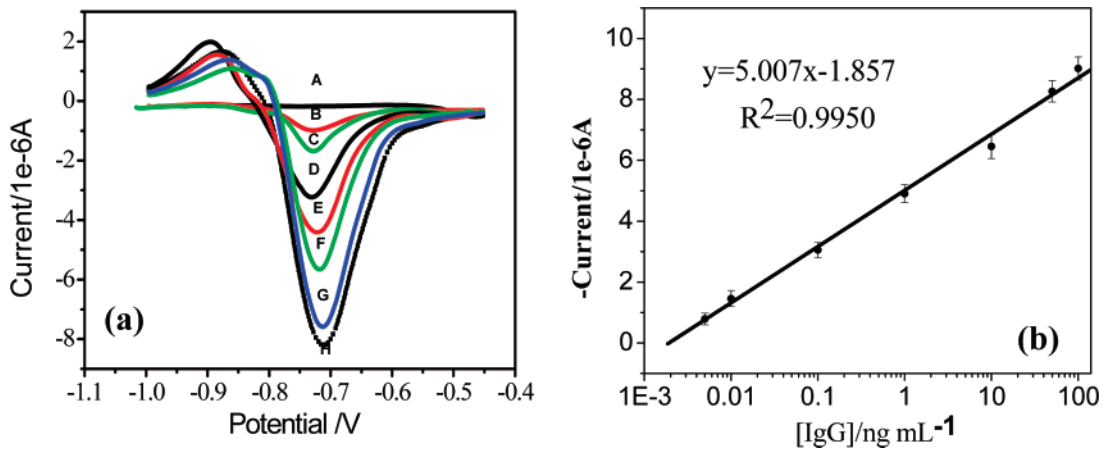

Figure 6. (a) Typical square wave voltammograms of electrochemical immunoassay with increasing HIgG concentration (from A to H: 0, 0.005, 0.01, 0.1, 1.0, 10, 50, and 100 ng mL^{-1} HIgG, respectively). (b) The resulting calibration curve of HIgG plotted on a semilog scale.

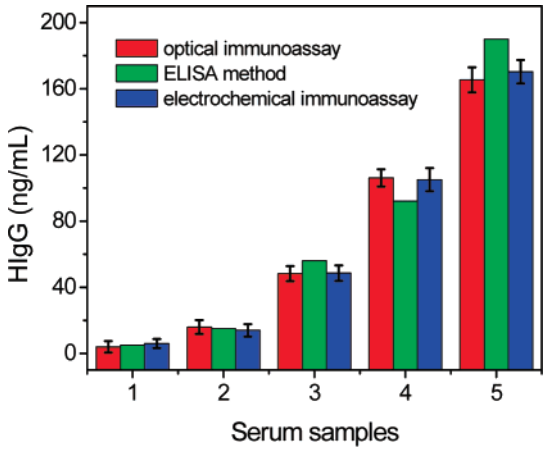

Figure 7. Comparison of serum HIgG levels determined using optical assay, electrochemical assay, and ELISA method.

correlation between the results obtained by optical immunoassay, electrochemical immunoassay, and the ELISA method. The relative deviations between optical assay and ELISA method were in the range of −10.9 to 10.3%, and the relative deviations between electrochemical assay and ELISA method were from −7.5 to 8.2%. It obviously indicates that there is no significant difference among the results given by three methods; that is, the developed versatile immunoassay may provide an interesting alternative tool for detection of protein in clinical laboratory.

Specificity, Regeneration, and Stability of the Immunosensor. Specificity is an important criterion for any analytical tool. The potential interference toward HIgG detection from coexisting species was studied with the versatile immunosensor. Using real samples containing 15.0 ng/mL C-reactive protein (CRP) and 15.0 ng/mL HIgG, the specificity of the proposed immunosensor was examined by detecting the fluorescence and electrochemical response, respectively. No significant difference of currents (RSD = 5.1%) and optical intensity (RSD = 6.2%) were observable in comparison with the result obtained in the presence of only HIgG (see Figure S1 in Supporting Information). The increase of CRP concentration to some extent did not lead to a significant signal change. Additionally, after the Ab_1/GNP-modified immunosensor was reacted with 10.0 ng/mL HIgG and QDs−Ab_2 followed by rinsing with stripping buffer of pH 3.5 glycine−hydrochloride to remove the Ag and QDs−Ab_2 from the immunocomplex, and the same immunosensor was reacted again with 10.0 ng/mL HIgG and QDs−Ab_2, the obtained fluorescence intensity and current signal restored 94 and 95% of the initial value after three assay runs. If the developed immunosensor was further treated with washing and sonication with detergent to detach all of the adsorbed PDDA, GNP, and biomolecules from the surface of ITO, it could be successively reused (see Figure S2 in Supporting Information). Thus, the immunosensor had a good specificity to HIgG as well as acceptable regeneration and reuse efficiency.

The performance stability of the Ab_1/GNP-modified ITO immunosensor was examined by storage in air, at room temperature, and at 4 °C, separately. The sensor lost its sensitivity rapidly if stored at room temperature. However, no obvious change was observed after 25-day storage at 4 °C (see Figure S2 in Supporting Information). This further indicated that a well-ordered GNP monolayer was very efficient for retaining the bioactivity and preventing the biomolecules from leaking out because of the strong interaction between GNP and mercapto or primary amine groups in these biomolecues.

CONCLUSION

It has been demonstrated here, for the first time, that CdTe QDs label was used as both electrochemical and optical signals for sensitive protein detection. A novel optical immunoassay based on gel imaging systems was developed to achieve a rapid analysis for the samples with a series of different concentrations of a target analyte in a single experiment. Electrochemical measurement was complementary to optical assay and offered high sensitivity. The sandwich-type immunosensor provided a convenient, low-cost, and versatile method for specific and highly sensitive detection of protein. This new assay can be applied to other biological assays, particularly DNA.

ACKNOWLEDGMENT

We greatly appreciate the support of the National Natural Science Foundation of China for distinguished Young Scholars

(20325516), the Key program (20635020), Creative Research Group (20521503), and General program (20575026). This work is also supported by National Basic Research Program of China (2006CB933201). The authors thank the European Commission Sixth Framework Program through a STREP grant to the SELECTNANO Consortium, Contract No. 516922, for financial support. The authors thank Prof. Jinan Zhang and Dr. Di Yang from Research Institute of Cardiovascular Disease of First Affiliated Hospital of Nanjing Medical University for their invaluable advice throughout the project.

SUPPORTING INFORMATION AVAILABLE

Additional information as noted in text. This material is available free of charge via the Internet at http://pubs.acs.org.

Received for review May 6, 2007. Accepted September 3, 2007.

AC070923D